Impact of molecular weight on the formation of electrosprayed chitosan microcapsules as delivery vehicles for bioactive compounds

Laura G. Gómez-Mascaraque[1], Gloria Sanchez[2,3], Amparo López-Rubio[1*]

[1]Food Quality and Preservation Department, IATA-CSIC, Avda. Agustin Escardino 7, 46980 Paterna, Valencia, Spain

[2]Department of Microbiology and Ecology, University of Valencia, Valencia, Spain

[3]Molecular Taxonomy Group, IATA-CSIC, Avda. Agustin Escardino 7, 46980 Paterna, Valencia, Spain

*Corresponding author: Tel.: +34 963900022; fax: +34 963636301 (A. López-Rubio)

E-mail addresses: lggm@iata.csic.es (L. G. Gómez-Mascaraque), gloriasanchez@iata.csic.es (G. Sanchez), amparo.lopez@iata.csic.es (A. López-Rubio)

[1] **Abbreviations**: ABTS, 2,2'-azino-bis(3-ethylbenzothiazoline-6-sulfonic acid) diammonium salt; DDA, degree of deacetylation DFA, Discriminant Function Analysis; EGCG, (–)-epigallocatechin gallate; FT-IR, Fourier transform infrared spectroscopy**;** GRAS, Generally Recognised As Safe; MEE, microencapsulation efficiency; MNV, murine norovirus; Mw, molecular weight(s); PBS, phosphate buffer saline; RSA, radical scavenging activity; SEM, scanning electron microscopy.

Abstract

The molecular weight of chitosan is one of its most determinant characteristics, which affects its processability and its performance as a biomaterial. However, information about the effect of this parameter on the formation of electrosprayed chitosan microcapsules is scarce. In this work, the impact of chitosan molecular weight on its electrosprayability was studied and correlated with its effect on the viscosity, surface tension and electrical conductivity of solutions. A Discriminant Function Analysis revealed that the morphology of the electrosprayed chitosan materials could be correctly predicted using these three parameters for almost 85% of the samples. The suitability of using electrosprayed chitosan capsules as carriers for bioactive agents was also assessed by loading them with a model active compound, (–)-epigallocatechin gallate (EGCG). This encapsulation, with an estimated efficiency of around 80% in terms of preserved antioxidant activity, showed the potential to prolong the antiviral activity of EGCG against murine norovirus via gradual bioactive release combined with its protection against degradation in simulated physiological conditions.

KEYWORDS

Electrospray; chitosan; molecular weight; microencapsulation; catechin; antiviral

1. Introduction

Micro- and nanoencapsulation, processes in which a compound is embedded within a protective matrix (Jiménez-Martín, Gharsallaoui, Pérez-Palacios, Carrascal & Rojas, 2014) which is organized in the form of micro- or nanosized structures, have attracted increasing research interest for the protection of sensitive bioactive compounds (Pérez-Masiá, López-Nicolás, Periago, Ros, Lagaron & López-Rubio, 2015) and address current concerns related to their formulation, bioavailability or their delivery to specific sites (Zaki, 2014).

Among the different techniques used for microencapsulation, electrohydrodynamic spraying (electrospraying) is rapidly emerging as a promising technology for the production of polymeric microparticles containing bioactive molecules (Bock, Dargaville & Woodruff, 2012), as it overcomes some of the limitations of conventional methods. Electrospraying can generate microencapsulation structures in a one-step process (Chakraborty, Liao, Adler & Leong, 2009) under mild conditions (López-Rubio & Lagaron, 2012; Sosnik, 2014) and in the absence of organic/toxic solvents (Tapia-Hernández et al., 2015), limiting inactivation of the bioactive compounds (Zamani, Prabhakaran & Ramakrishna, 2013), being adequate for both hydrophilic and hydrophobic drugs or ingredients (Gómez-Mascaraque & López-Rubio, 2016) and generally achieving high loading efficiencies (Sosnik, 2014; Zamani, Prabhakaran & Ramakrishna, 2013). Therefore, it has found a number of potential applications in various fields, including the pharmaceutical, cosmetic and food industries (Jaworek & Sobczyk, 2008). It basically consists on subjecting a polymer solution (containing the bioactive to be encapsulated) to a high voltage so that the electric field deforms the interface of the liquid drop and breaks it into fine charged droplets, which are ejected

towards a collector while the solvent evaporates, generating dry polymeric microparticles (Anu Bhushani & Anandharamakrishnan, 2014; Sosnik, 2014).

Biopolymers are preferred as encapsulating matrices for most applications because of their biocompatibility, biodegradability and non-toxicity (Ghorani & Tucker, 2015). Specially, chitosan is a biorenewable, biocompatible and biodegradable polysaccharide considered a GRAS food additive by the FDA (Luo & Wang). Moreover, it has many attributed functional and bioactive properties, including antioxidant and lipid-lowering capacities, antimicrobial activity, wound healing and antiangiogenic effects, prevention of renal failure, etc. (Luo & Wang; Park, Saravanakumar, Kim & Kwon, 2010; Ribeiro et al., 2009). For these reasons chitosan and its derivatives have been widely used in the pharmaceutical (Badwan, Rashid, Omari & Darras, 2015; Cheung, Ng, Wong & Chan, 2015), biomedical (Anitha et al., 2014; Ishihara, 2015), cosmetic (Anumansirikul, 2007; Jimtaisong & Saewan, 2014) and food industries (Fathi, Martin & McClements, 2014; Zivanovic, Davis & Golden, 2014), and is considered a good candidate for the encapsulation of bioactive compounds (Estevinho, Rocha, Santos & Alves, 2013; Varshosaz, 2007). However, the electrohydrodynamic processing of chitosan is complex due to its particular behavior in solution and its polycationic nature (Homayoni, Ravandi & Valizadeh, 2009), consequence of its structure consisting of β-1,4 linked 2-acetamido-2-deoxy-β-D-glucopyranose units and 2-amino-2-deoxy-b-D-glucopyranose units (cf. Figure S1 of the Supplementary Material) (Khor & Lim, 2003).

The electrohydrodynamic spinning (electrospinning) of chitosan for the production of nanofibers from non-toxic solvents has been extensively studied (Sun & Li), and the impact of different processing parameters, solution properties and/or the molecular weight of the polymer on the morphology of the obtained fibers have been addressed (Geng, Kwon & Jang, 2005; Homayoni, Ravandi & Valizadeh, 2009). However, as the

84 focus of these works is the manufacture of fibers, the range of explored conditions does
85 not cover the production of nano/microparticles. The use of electrospraying for the
86 production of dry (Arya, Chakraborty, Dube & Katti, 2009; Zhang & Kawakami, 2010)
87 or gelled (Pancholi, Ahras, Stride & Edirisinghe, 2009; Wang et al., 2015; Yunoki,
88 Tsuchiya, Fukui, Fujii & Maruyama, 2014) chitosan micro- and nanospheres has also
89 been reported, however, all these works use only one particular grade of chitosan, with a
90 fixed molecular weight. Given that the molecular weight of chitosan is one of its key
91 characteristics, which can affect not only its processability but also its performance as a
92 delivery vehicle (Arya, Chakraborty, Dube & Katti, 2009), the focus of this work was to
93 study the influence of the molecular weight on the sprayability of chitosan, and to assess
94 the suitability of selected electrosprayed capsules as delivery vehicles for a model
95 bioactive compound: (–)-epigallocatechin gallate (EGCG). EGCG is the most abundant
96 and bioactive compound in green tea (Barras et al., 2009) and possesses many attributed
97 health benefits (Singh, Shankar & Srivastava, 2011), including protective effects against
98 infections (Steinmann, Buer, Pietschmann & Steinmann, 2013), cardiovascular and
99 neurodegenerative diseases (Fu et al., 2011), inflammation and arthritis (Singh, Akhtar
100 & Haqqi, 2010) and cancer (Larsen & Dashwood, 2009, 2010). In the present work, its
101 antioxidant (Fu et al., 2011) and antiviral (Dhiman, 2011; Xiao, 2008) activities were
102 assessed before and after encapsulation within the chitosan electrosprayed capsules.

103

104 **2. Materials and Methods**

105 **2.1. Materials**

106 Chitosans with reported degree of deacetylation of 85 ± 2.5 % and different molecular
107 weights, ranging from 25 to 300 kDa, were purchased from Heppe Medical Chitosan

GmbH. (–)-Epigallocatechin gallate (EGCG), 2,2'-azino-bis(3-ethylbenzothiazoline-6-sulfonic acid) diammonium salt (ABTS), potassium persulfate ($K_2O_8S_2$) and spectroscopic grade potassium bromide (KBr) were obtained from Sigma-Aldrich. 96% (v/v) acetic acid was supplied by Scharlab.

2.2. Preparation of chitosan solutions

Chitosan solutions of different concentrations, i.e. from 0.5 to 8 % (w/v), were prepared by dissolving the polysaccharide in acetic acid at room temperature under magnetic agitation overnight. Different acetic acid concentrations were used for this purpose, from 20 to 90 % (v/v).

2.3. Characterization of the solutions

The surface tension of the solutions was measured using the Wilhemy plate method in an EasyDyne K20 tensiometer (Krüss GmbH, Hamburg, Germany) at room temperature.

The electrical conductivity of the solutions was measured using a conductivity meter XS Con6 (Labbox, Barcelona, Spain) at room temperature.

The rheological behaviour of the solutions was studied using a rheometer model AR-G2 (TA Instruments, USA), with a parallel plate geometry, and the method described in (Gómez-Mascaraque, Lagarón & López-Rubio, 2015). Briefly, continuous shear rate ramps were performed from 0.1 to 200 s^{-1} during 15 min at 25 ± 0.1 ºC using a stainless

steel plate with a diameter of 60 mm and a gap of 0.5 mm. All measurements were made at least in triplicate.

2.4. Electrohydrodynamic processing of the solutions

The solutions were processed using a homemade electrospinning/electrospraying apparatus, equipped with a variable high-voltage 0-30 kV power supply. Solutions were introduced in a 5 mL syringe and were pumped at a steady flow-rate (0.15 mL/h) through a stainless-steel needle (0.9 mm of inner diameter). The needle was connected through a PTFE wire to the syringe, which was placed on a digitally controlled syringe pump. Processed samples were collected on a grounded stainless-steel plate placed at a distance of 10 cm from the tip of the needle in a horizontal configuration. A voltage of 17 kV was applied to the solutions as selected in preliminary trials.

2.5. Morphological characterization of the particles

Scanning electron microscopy (SEM) was conducted on a Hitachi microscope (Hitachi S-4800) at an accelerating voltage of 10 kV and a working distance of 7-10 mm. As prepared samples were sputter-coated with a gold-palladium mixture under vacuum prior to examination.

2.6. Fourier transform infrared (FT-IR) analysis of the particles

Samples (ca. 1-2 mg) of selected chitosan capsules, both unloaded and EGCG-loaded, were grounded and dispersed in about 130 mg of spectroscopic grade potassium

bromide (KBr). A pellet was then formed by compressing the samples at ca. 150 MPa. FT-IR spectra were collected in transmission mode using a Bruker (Rheinstetten, Germany) FT-IR Tensor 37 equipment. The spectra were obtained by averaging 10 scans at 1 cm^{-1} resolution.

2.7. Antioxidant activity of free and encapsulated EGCG

The $ABTS^{+\bullet}$ radical scavenging assay (Re, Pellegrini, Proteggente, Pannala, Yang & Rice-Evans, 1999) was performed in order to quantify the antioxidant activity of both free and encapsulated EGCG, following the protocol described in a previous work (Gómez-Mascaraque, Lagarón & López-Rubio, 2015). Briefly, a stock solution of $ABTS^{+\bullet}$ was prepared by reacting ABTS 7 mM with potassium persulfate 2.45 mM, both in distilled water, and allowing the mixture to stand in the dark at room temperature for 24 h. The stock solution was then diluted with acetic acid 20% v/v to an absorbance at 734 nm of 0.70 ± 0.02. Solutions of free and encapsulated EGCG (0.15 mg/mL of EGCG in both cases) were prepared in acetic acid 20% v/v, and 10 µL aliquots were added to 1 mL of diluted $ABTS^{+\bullet}$, measuring its absorbance at 734 nm after 1 min of mixing. The unloaded chitosan particles were also evaluated, at the same polymer concentration as for the loaded samples. The radical scavenging activity (RSA), expressed as the percentage of reduction of the absorbance at 734 nm after sample addition, was calculated using Eq. (1), where A_0 and A_1 are the absorbances at 734 nm of $ABTS^{+\bullet}$ before and 1 min after addition of the samples, respectively.

$$\text{RSA}\ (\%) = \frac{A_0 - A_1}{A_0} \times 100 \qquad \text{Eq. (1)}$$

Experiments were performed on a V-1200 Spectrophotometer from VWR (Pennsylvania, USA), at least in triplicate. Solvent blanks were also run in each assay.

2.8. Microencapsulation efficiency

The microencapsulation efficiency (MEE) of the EGCG-loaded capsules was estimated from the value of their antioxidant activity according to Eq. (2), where both the free and encapsulated EGCG had the same theoretical concentration in the solutions:

$$MEE\ (\%) = \frac{RSA\ of\ EGCG{-}loaded\ capsules}{RSA\ of\ free\ EGCG} \times 100 \qquad \text{Eq. (2)}$$

2.9. Virus strain, cell line and infections

The cytopathogenic murine norovirus (MNV-1) strain, a model for human noroviruses, was propagated and assayed in RAW 264.7 (kindly provided by Prof. H. W. Virgin, Washington University School of Medicine, USA) as described in Elizaquível, Azizkhani, Aznar and Sánchez (2013). Semi-purified stocks were subsequently produced from the same cells by centrifugation of infected cell lysates at 660×g for 30 min. Infectious viruses were enumerated by determining the 50% tissue culture infectious dose ($TCID_{50}$) with eight wells per dilution and 20 µl of inoculum per well.

2.10. Antiviral activity

Different concentrations of free and encapsulated EGCG were added to MNV suspensions (ca. 6 log $TCID_{50}$/mL) and further incubated at 37 °C in a water-bath

198 shaker at 150 rpm for 2 or 16 h (ON). Ten-fold dilutions of treated and untreated virus
199 suspensions were inoculated into confluent RAW monolayers in 96-well plates. Then,
200 infectious viruses were quantified by cell culture assays as described above. Each
201 treatment was done in triplicate. Positive controls were virus suspensions in PBS and
202 virus suspensions added to unloaded chitosan capsules. The decay of MNV was
203 calculated as $\log_{10}(N_t/N_0)$, where N_0 is the infectious MNV titer for untreated sample
204 and N_t is the infectious MNV titer for treated samples.

205

206 **2.11. Statistical analysis**

207 A statistical analysis of experimental data was performed using IBM SPSS Statistics
208 software (v.23) (IBM Corp., USA). Significant differences between homogeneous
209 sample groups were obtained through two-sided t-tests (means test of equality) at the
210 95% significance level ($p < 0.05$). For multiple comparisons, the p-values were adjusted
211 using the Bonferroni correction. This software was also used to carry out a Discriminant
212 Function Analysis (DFA) (cf. Section 3.2.3).

213

214 **3. Results and discussion**

215 **3.1. Impact of the molecular weight on the morphology of electrosprayed chitosan**
216 The use of electrospraying for the production of chitosan micro- and nanospheres for
217 drug delivery applications, and the influence of different processing parameters on the
218 obtained materials has already been reported for specific chitosans (Arya, Chakraborty,
219 Dube & Katti, 2009; Maeng, Choi, Kim & Kim, 2010; Pancholi, Ahras, Stride &
220 Edirisinghe, 2009; Yunoki, Tsuchiya, Fukui, Fujii & Maruyama, 2014; Zhang &

221 Kawakami, 2010). However, there is lack of information about the influence that the
222 molecular weight of chitosan itself has on the morphology of the materials obtained
223 through electrospraying. Thus, the formation of microencapsulation structures through
224 electrospinning/electrospraying using different chitosans with varying molecular
225 weights (Mw) and in a wide range of concentrations was evaluated under the same
226 processing conditions (i.e. an applied voltage of 17 kV, a flow rate of 0.15 mL/h and a
227 needle-collector distance of 10 cm), which were selected in preliminary trials so as to be
228 able to process all the solutions. The mean degree of deacetylation (DDA) of all
229 chitosans was 85% (± 2.5 %), and they were all dissolved in 90% acetic acid based on
230 previous works (Arya, Chakraborty, Dube & Katti, 2009; Pérez-Masiá, Lagaron &
231 Lopez-Rubio, 2015; Zhang & Kawakami, 2010). Figure 1 summarizes the types of
232 morphologies obtained for the different Mw-concentration pairs tested, showing the
233 micrographs obtained by SEM for some representative samples.

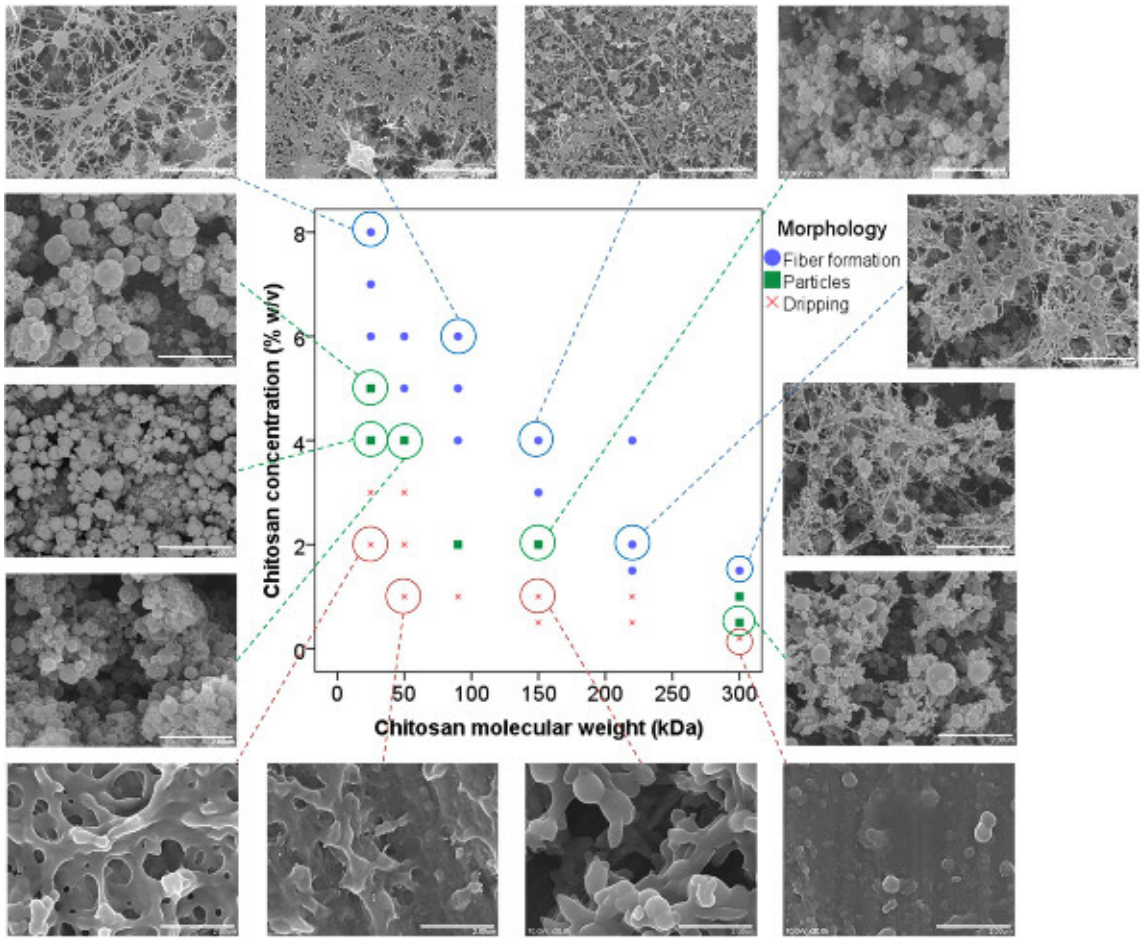

Figure 1. Combined effect of molecular weight and concentration on the morphology of electrosprayed chitosan materials. White scale bars in all the SEM micrographs represent 2 µm.

The results revealed that there was a small range of Mw-concentration conditions which yielded neat electrosprayed particles under the selected processing parameters. Small deviations from these conditions either caused fiber formation or dripping of the chitosan solutions. As expected, an increase in the molecular weight of chitosan caused a decrease in the concentration at which it could be successfully electrosprayed. Indeed, as the molecular weight of a polymer increases, so does the frequency of chain entanglements and thus the intermolecular cohesion in solution for a fixed concentration. The formation of chain entanglements has been acknowledged as the main factor determining the different morphologies which can be obtained when a polymer solution is processed electrohydrodynamically (Shenoy, Bates, Frisch & Wnek, 2005). Accordingly, when a sufficient entanglement concentration is reached, jet fragmentation during processing is prevented and fibers are formed (Gómez-

249 Mascaraque, Lagarón & López-Rubio, 2015). In a polymer solution, the number of
250 chain entanglements is affected both by the concentration and the molecular weight of
251 the polymer (Shenoy, Bates, Frisch & Wnek, 2005), and is related to the viscosity of
252 the solutions (Cross, 1970). Thus, in order to better understand the influence of the
253 molecular weight on the morphology of the processed materials, the rheological
254 behaviour of the chitosan solutions was examined, together with other solution
255 properties (surface tension and electrical conductivity) that are known to strongly
256 impact electrohydrodynamic processing (Pérez-Masiá, Lagaron & López-Rubio, 2014).

257

258 **3.2. Chitosan solution properties**

259 **3.2.1. Rheological behaviour**

260 In general, the most diluted chitosan solutions exhibited a Newtonian behavior, with a
261 linear relationship between the shear stress (σ) and the shear rate ($\dot{\gamma}$), regardless of the
262 molecular weight of the polymers. However, as the concentration increased, the
263 chitosan samples showed a shear thinning (pseudoplastic) behavior as previously
264 reported (Iversen, Kjøniksen, Nyström, Nakken, Palmgren & Tande, 1997), which was
265 manifested at lower concentrations for the higher molecular weight chitosans, and was
266 more evident as both the chitosan concentration and its molecular weight increased.
267 Figure S2 of the Supplementary Material shows the rheological profiles obtained for
268 different concentrations of chitosan with a molecular weight of 150 kDa, as a
269 representative example. In order to compare the viscosity of the different chitosan
270 solutions, its value at a constant high shear rate (200 s^{-1}) was plotted against the
271 polymer concentration for each molecular weight (cf. Figure 2). As predicted by Al-
272 Fariss and Al-Zahrani (1993) for diluted polymer solutions, the viscosity exponentially
273 increased with the concentration of chitosan at a constant temperature and shear rate,

while a potential relationship of the viscosity of chitosan solutions with its molecular weight was observed (cf. Figure S3 of the Supplementary Material) as predicted by the Mark–Houwink equation (Kasaai, 2007; Wang, Bo, Li & Qin, 1991). Overall, the viscosity could be increased either by increasing the concentration or the mean molecular weight of the polysaccharide, as expected. However, the values of the viscosity alone did not explain the different morphologies obtained, as the ranges of this parameter which yielded neat particles, particles with fibers or just dripping of the solution overlapped (cf. Figure S4 of the Supplementary Material).

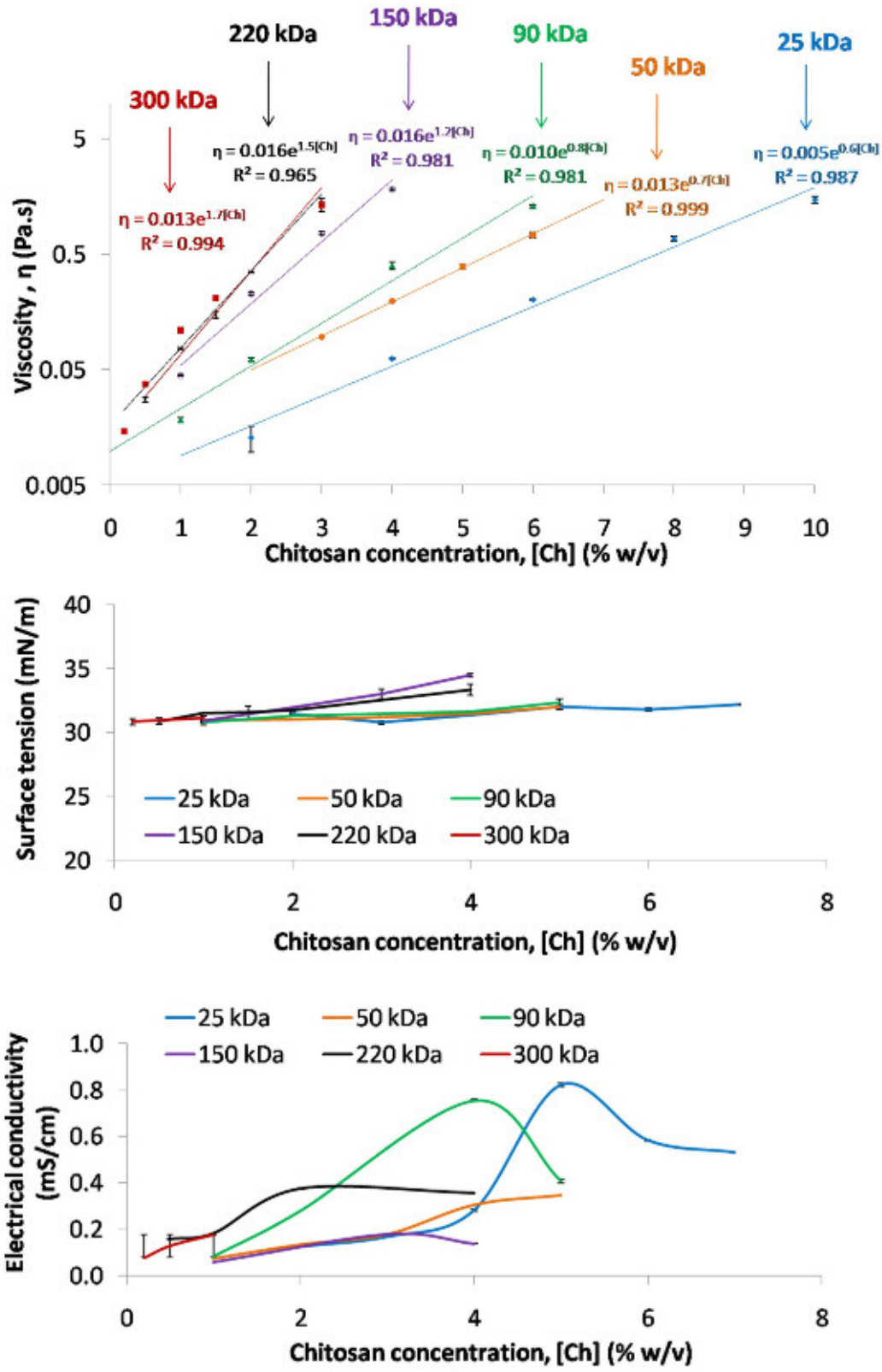

Figure 2. Viscosity, surface tension and electrical conductivity of chitosan solutions as a function of the polymer concentration for different molecular weights.

3.2.2. Surface tension and electrical conductivity

The surface tension of the chitosan solutions hardly varied with the molecular weight or the concentration of the polysaccharide, increasing only slightly as both increased (cf. Figure 2). This lack of substantial variation with the concentration of biopolymer has also been observed for other systems (Gómez-Mascaraque, Lagarón & López-Rubio, 2015).

The electrical conductivity initially increased with chitosan concentration for the different molecular weights evaluated but eventually showed a maximum for the lower Mw chitosans, i.e. for the solutions where the viscosity allowed evaluation of a wider range of concentrations (cf. Figure 2). This can be explained taking into account that the conductivity depends on both the concentration of charges and their mobility. As the concentration of chitosan, and thus of protonated amino groups increased, the conductivity augmented up to a point when the viscosity was so high that the mobility of the charges was hampered. Indeed, these maximum was found at higher concentrations for lower molecular weights. It was interesting to find that the concentration at which each chitosan grade was successfully electrosprayed in the form of neat particles had an electrical conductivity in the increasing slope of the curves, before the maximum, because the viscosity at higher concentrations was too high and gave rise to fibrils.

Anyhow, as expected, none of the solution properties could explain the differences in the morphology of the obtained materials on its own. In contrast, a combination of them could help predicting the sprayability of chitosan with a specific molecular weight at a particular concentration.

3.2.3. Combined effect of the solution properties on the morphology

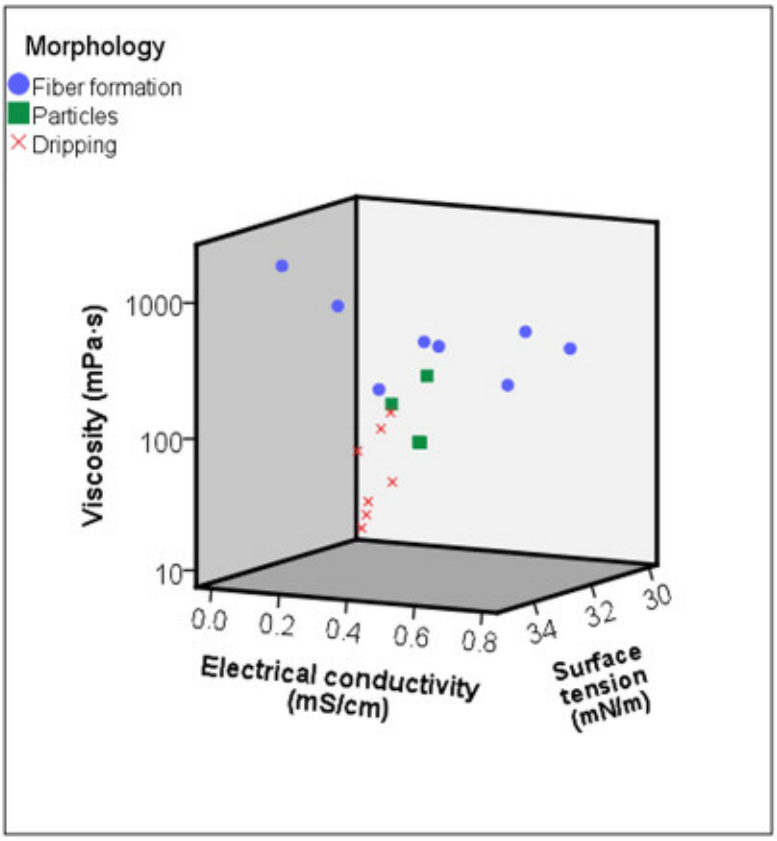

Figure 3. Electrosprayed samples classified by their morphology as a function of the solution properties

Figure 3 shows the small region where the confluence of certain viscosity, surface tension and electrical conductivity values yielded electrosprayed particles free of residual fibrils. In order to ascertain whether these three properties were effective in predicting the morphology of the electrosprayed materials, a Discriminant Function Analysis (DFA) was conducted using the software IBM SPSS Statistics (v.23). This type of statistical analysis is used to determine if a definite set of variables is successful in predicting a category membership (Rencher, 1992). The DFA revealed that the three variables were relevant to discriminate the different structures. The best rate of discrimination was obtained using the combinations of the variables expressed in Eq. (3) and (4) as standardized canonical discriminant functions, where γ is the surface

tension expressed in mN/m, κ is the electrical conductivity expressed in (mS/cm) and η is the viscosity expressed in Pa·s.

$$Function\ 1 = -0.032 \cdot \gamma + 0.462 \cdot \kappa + 0.928 \cdot \log(\eta) \quad \text{Eq. (3)}$$

$$Function\ 2 = 1.365 \cdot \gamma + 0.0128 \cdot \kappa - 0.811 \cdot \log(\eta) \quad \text{Eq. (4)}$$

With the above discriminant functions, the morphology obtained upon electrospraying of chitosan solutions could be correctly predicted for 84.2% of the assayed solutions (cf. Figure 4). Moreover, all solutions leading to neat particles were correctly classified.

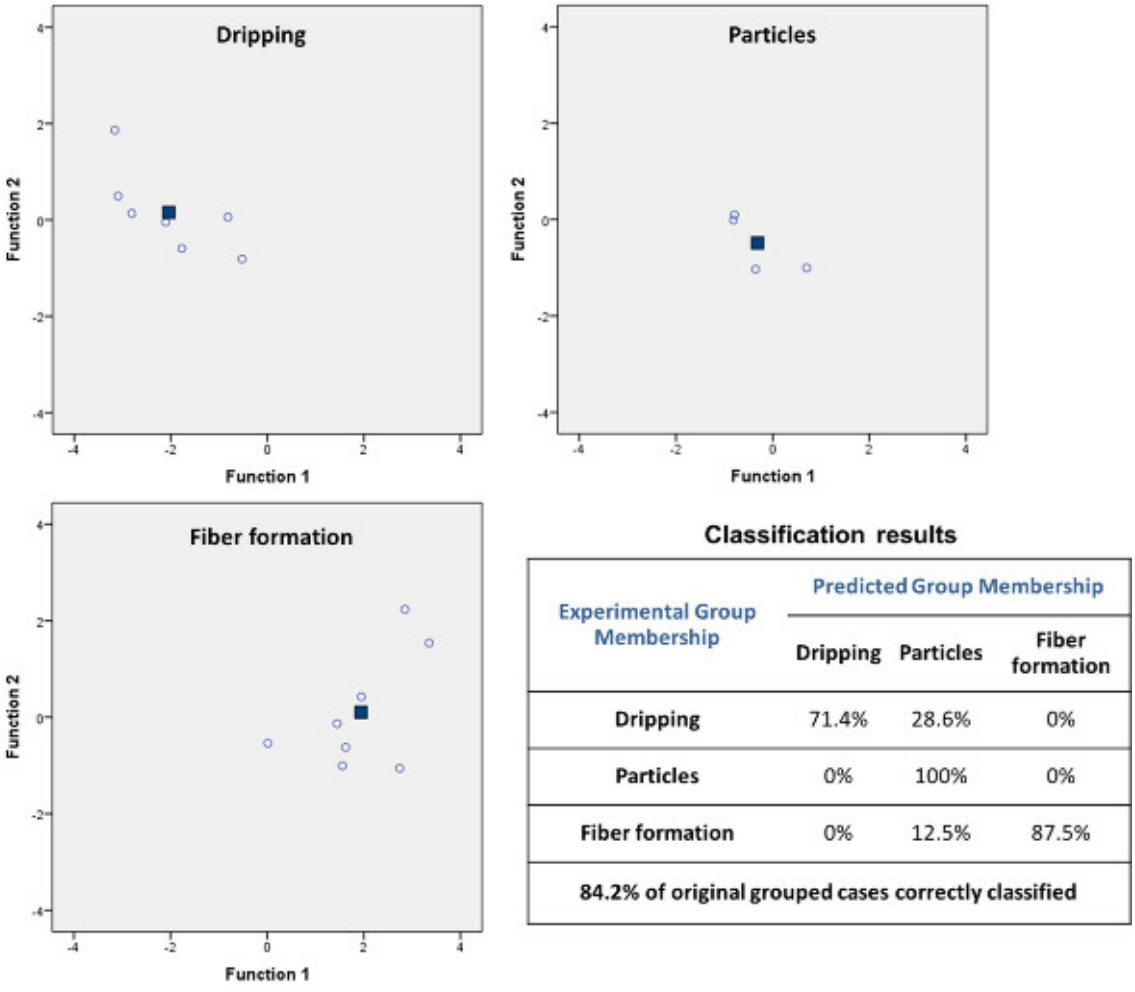

Classification results

Experimental Group Membership	Predicted Group Membership		
	Dripping	Particles	Fiber formation
Dripping	71.4%	28.6%	0%
Particles	0%	100%	0%
Fiber formation	0%	12.5%	87.5%
84.2% of original grouped cases correctly classified			

Figure 4. Group graphs obtained from the discriminant functions (Eq. (3) and (4)) and classification results

From the different molecular weight – concentration combinations which gave rise to fiber-free electrosprayed particles, the chitosan with the lowest assayed molecular weight was selected, as it allowed the highest electrosprayable concentration and thus the greatest productivity. Thus, the chitosan of 25 kDa at 5% (w/v) concentration was selected for further analysis.

3.3. Effect of acetic acid concentration

One of the solution parameters that are crucial for the electrohydrodynamic processing of chitosan solutions is the concentration of the acetic acid solution used as solvent. While Homayoni, Ravandi and Valizadeh (2009) stated that the acetic acid concentration should be in the range of 70-90% for optimal electrospinning to obtain nanofibers, Arya, Chakraborty, Dube and Katti (2009) concluded that the optimum concentration for successful electrospraying was 90%, though that might only apply for the particular chitosan they used. This concentration has been selected in other works to produce electrosprayed particles from chitosan (Pérez-Masiá, Lagaron & Lopez-Rubio, 2015; Sun et al., 2015) without further evaluation. However, Zhang and Kawakami (2010) extended the range of sprayability (again, for a particular chitosan of high molecular weight) down to a 50%, noting that decreasing the acetic acid concentration caused a reduction in the mean particle size. Due to the variability of data found in the literature in this respect, the concentration of acetic acid was optimized for our particular system (chitosan 25 kDa, 5% w/v).

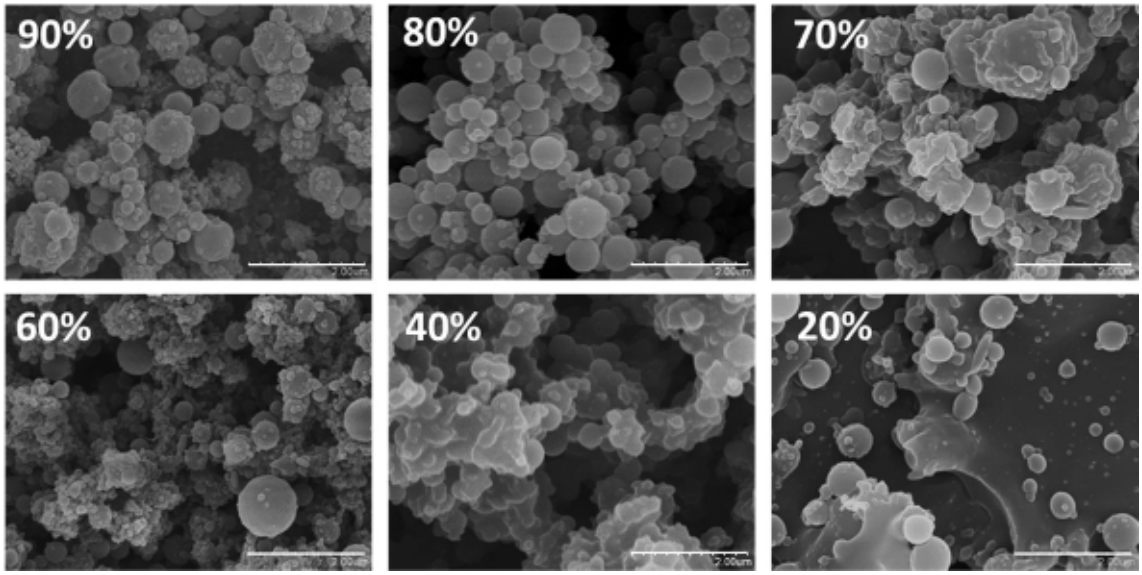

Figure 5. Morphology of electrosprayed chitosan (25 kDa, 5% w/v) obtained from different acetic acid concentrations (90-20% v/v). White scale bars in all the SEM micrographs represent 2 µm.

Figure 5 shows the impact of the acetic acid concentration on the morphology of the electrosprayed chitosan. It could be observed that concentrations below 80% yielded particle aggregates and even dripping of the solution for a 20% acetic acid. As the surface tension of the solutions did not vary significantly with the acetic acid concentration (cf. Figure S5 of the Supplementary Material), this dripping could be attributed to a slight decrease in the viscosity of the solutions in combination with a sharp increase in their electrical conductivity at low acetic concentrations, which had already been observed by Zhang and Kawakami (2010) and ascribed to the higher degree of dissociation of the acid at low concentrations. However, a concentration of 80% gave rise to more spherical particles with more homogeneous sizes than the 90% used in the previous sections. Having both concentrations the same conductivity, this was attributed to the maximum of viscosity observed at 80% acetic acid (cf. Figure S5 of the Supplementary Material), also patent in the cited work (Zhang & Kawakami, 2010) although not commented. Therefore, an optimum acetic acid concentration of 80% was selected to produce our delivery system.

3.4. Morphological and chemical characterization of EGCG-loaded capsules

The conditions selected in the previous section for the production of electrosprayed chitosan delivery vehicles where used to produce EGCG-loaded chitosan particles with a theoretical EGCG content of 10% w/w of the capsules. Figure 6(a) shows a micrograph of the obtained material, which exhibits a similar morphology as that obtained in the absence of the bioactive compound, although slightly less homogeneous in size.

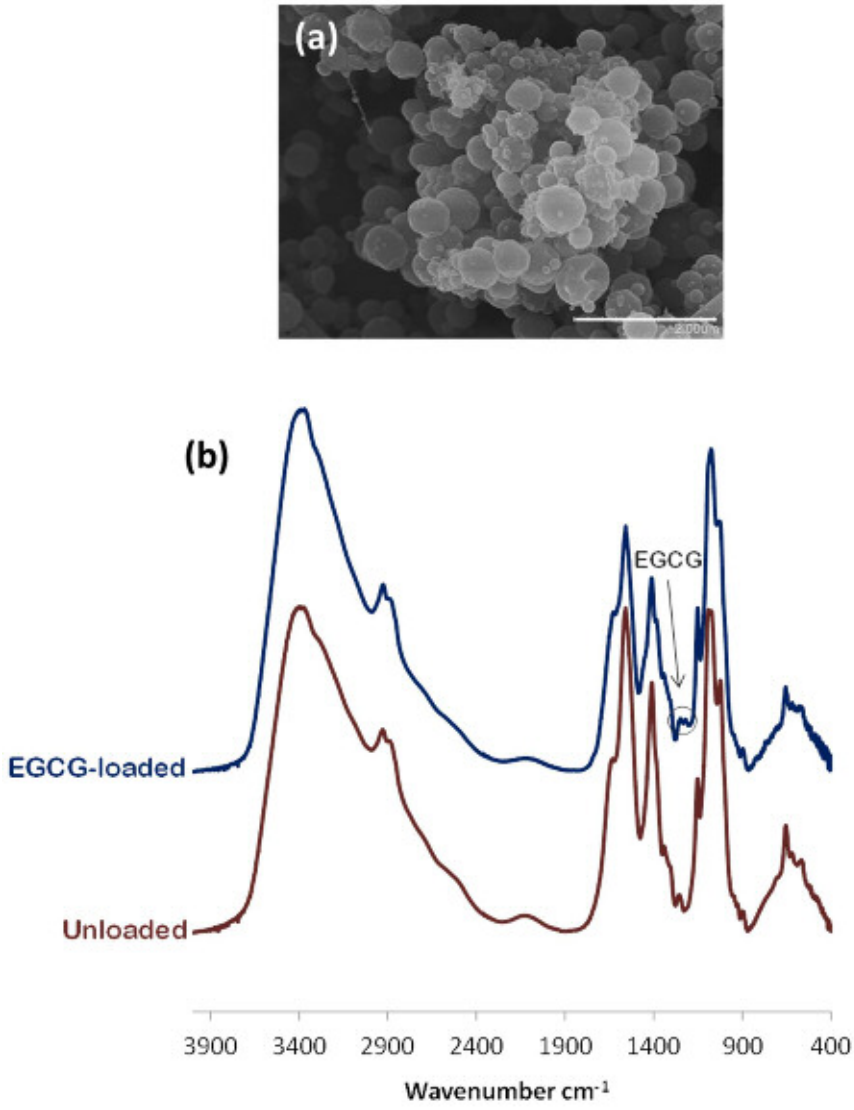

386 **Figure 6. Morphology of EGCG-loaded electrosprayed chitosan particles (a) and infrared spectra**
387 **of unloaded and EGCG-loaded electrosprayed chitosan particles (b). The white scale bar in the**
388 **SEM micrograph represents 2 μm.**

389

390 The effective incorporation of EGCG within the chitosan particles was evidenced by the
391 presence of its characteristic infrared absorption band centred at 1221 cm^{-1} (cf. Figure
392 6(b)), as observed for EGCG-loaded spray-dried chitosan particles obtained in a
393 previous work (Gómez-Mascaraque, Soler & López-Rubio, 2016). This band was
394 slightly displaced in the capsules with respect to free EGCG, being centred at 1223 cm^{-1}
395 in the latter (spectrum showed elsewhere (Gómez-Mascaraque, Lagarón & López-
396 Rubio, 2015)). Other spectral bands of chitosan were also modified. Specifically, the
397 Amide I band shifted from 1634 cm^{-1} in the unloaded particles to 1629 cm^{-1} in the
398 EGCG-loaded capsules. These changes suggested the presence of intermolecular
399 interactions between the bioactive molecule and its biopolymeric vehicle, which might
400 contribute to the stabilization of the former as previously suggested (Gómez-
401 Mascaraque, Lagarón & López-Rubio, 2015).

402

403 **3.5. Antioxidant activity and encapsulation efficiency**

404 The ABTS radical cation decolourization assay (Re, Pellegrini, Proteggente, Pannala,
405 Yang & Rice-Evans, 1999) was used to compare the antioxidant activity of free and
406 encapsulated EGCG, and to indirectly estimate the encapsulation efficiency of the
407 system. Therefore, the radical scavenging activities (RSA) of solutions of commercial
408 EGCG (0.15 mg/mL) and encapsulated EGCG (theoretical concentration of 0.15
409 mg/mL) in acetic acid 20% v/v, as well as solutions of the unloaded chitosan particles
410 (same concentration as for the loaded ones) were calculated using Eq. (1). Solvent
411 blanks were run too.

412 The results showed no significant differences ($p<0.05$) between the RSA of the
413 unloaded chitosan particles (2.3% ± 0.3%) and that of the solvent blank (2.2% ± 0.4%),
414 suggesting that the polysaccharide exerted no significant antioxidant activity at the
415 assayed concentration. Hence, the potential contribution of the encapsulating matrix to
416 the total antioxidant activity of the EGCG-loaded capsules was neglected. The
417 antioxidant activity of encapsulated EGCG (RSA = 23.0% ± 0.7%) was somewhat
418 lower than that of free EGCG (RSA = 28.9% ± 1.7%) at the same theoretical
419 concentration, implying some bioactivity loss during encapsulation.

420 From these results, the encapsulation efficiency defined by Eq. (2) was estimated to be
421 79.6% ± 2.4%. This considerably high value was consistent with similar encapsulation
422 systems based on chitosan used as delivery vehicles for EGCG (Gómez-Mascaraque,
423 Soler & López-Rubio, 2016).

424

425 **3.6. Antiviral activity**

426 Table 1 summarizes the results obtained from the antiviral activity assays performed on
427 murine norovirus. While a concentration of 0.25 mg/mL of EGCG was insufficient to
428 observe a significant reduction in the recovered titer of the virus after 2 h of incubation,
429 a concentration of 2.5 mg/mL of the polyphenol did cause a significant reduction, which
430 was statistically lower for the encapsulated compound suggesting that 2 h was
431 insufficient for the complete release of the bioactive. On the contrary, when the viruses
432 were exposed to EGCG overnight, the recovered titer was lower than 1.15 $TCID_{50}$/mL
433 for both free and encapsulated EGCG at 2.5 mg/mL and, more interestingly, the
434 reduction was significantly higher for the encapsulated than for the free flavonoid at
435 0.25 mg/mL.

436

437 **Table 1. Antiviral activity of free and encapsulated EGCG against murine norovirus**

	[Sample] (mg/mL)	Theoretical [EGCG] (mg/mL)	2 h		Overnight	
			Recovered titer ($TCID_{50}$/mL)	Reduction	Recovered titer ($TCID_{50}$/mL)	Reduction
PBS	-		6.45 ± 0.35^{A}	-	5.87 ± 0.38^{A}	-
Free EGCG	2.5	2.5	4.13 ± 0.10^{B}	2.32	$<1.15^{B}$	>4.72
	0.25	0.25	6.03 ± 0.12^{A}	0.42	4.71 ± 0.12^{C}	1.16
EGCG-loaded chitosan	25	2.5	5.20 ± 0.00^{C}	1.25	$<1.15^{B}$	>4.72
	2.5	0.25	6.07 ± 0.21^{A}	0.38	3.48 ± 0.38^{D}	2.39

438 * **Within each column, different letters (A, B, C and D) denote significant differences between**
439 **treatments ($p < 0.05$).**

440

441 Given that the unloaded electrosprayed chitosan did not show antiviral activity (data not
442 shown), these results can be explained considering that the bioactive compound might
443 have been gradually released from the microcapsules. In fact, a sustained release of
444 bioactives is often desirable and pursued through their encapsulation (Singh, 2010). In
445 our system, the lower antiviral activity of encapsulated EGCG at short exposure times
446 and its substantial increase at longer time periods suggested a gradual release of the
447 active compound from the chitosan capsules, mainly ascribed to a Fickian diffusion
448 mechanism with some contribution from polymer relaxation phenomena. This result is
449 consistent with the release profiles obtained for similar systems based on EGCG-loaded
450 chitosan microcapsules (Gómez-Mascaraque, Soler & López-Rubio, 2016). On the
451 other hand, the fact that the reduction in the recovered titer was higher for the
452 encapsulated EGCG after an overnight incubation implied that free EGCG was less
453 active against the MNV than the EGCG released from the capsules. As the assay was

carried out in PBS at 37ºC to mimic physiological conditions, this can be easily explained by the great instability of EGCG in slightly alkaline solutions (Sang, Lee, Hou, Ho & Yang, 2005; Su, Leung, Huang & Chen, 2003; Wang, Zhou & Wen, 2006). Therefore, the results suggested that while free EGCG degraded with time in PBS, microencapsulation of the compound within the electrosprayed chitosan particles delayed its degradation, hence protecting its antiviral activity in simulated physiological conditions.

4. Conclusions

There was a small range of molecular weight – concentration combinations which gave rise to electrosprayed particles without leading to solution dripping or fiber formation. Both parameters caused a considerable increase in the viscosity of the solutions, although the values of the viscosity on their own were not enough to predict whether a particular chitosan solution would lead to fiber-free particles. A Discriminant Function Analysis revealed that the surface tension and the electrical conductivity of the solutions were also relevant properties in predicting the obtained morphologies. The analysis allowed the accurate prediction of 84.2% of the electrosprayed chitosan solutions. The chitosan with the lowest assayed molecular weight (25 kDa), which allowed the highest electrosprayable concentration (5% w/v) and thus the highest productivity, was used to produce EGCG-loaded encapsulation structures achieving an encapsulation efficiency close to 80%. Microencapsulated EGCG showed prolonged antiviral activity against murine norovirus as compared to the free compound, suggesting that EGCG was gradually released from the chitosan capsules and that the encapsulation matrix exerted

a protective effective on the active compound against degradation in simulated physiological conditions.

Acknowledgements

Laura G. Gómez-Mascaraque is recipient of a predoctoral contract from the Spanish Ministry of Economy and Competitiveness (MINECO), Call 2013. Gloria Sanchez was supported by the "Ramón y Cajal" Young Investigator Program. The authors would like to thank the Spanish MINECO project AGL2015-63855-C2-1 and INIA grant RTA2014-00024-C04-03 for financial support. Authors would also like to thank the Central Support Service for Experimental Research (SCSIE) of the University of Valencia for the electronic microscopy service.

References

Al-Fariss, T., & Al-Zahrani, S. (1993). Rheological behaviour of some dilute polymer solutions. *Engineering Sciences, 5*(1).

Anitha, A., Sowmya, S., Kumar, P. T. S., Deepthi, S., Chennazhi, K. P., Ehrlich, H., Tsurkan, M., & Jayakumar, R. (2014). Chitin and chitosan in selected biomedical applications. *Progress in Polymer Science, 39*(9), 1644-1667.

Anu Bhushani, J., & Anandharamakrishnan, C. (2014). Electrospinning and electrospraying techniques: Potential food based applications. *Trends in Food Science & Technology, 38*(1), 21-33.

Anumansirikul, N. (2007). *Chitosan-nanoparticles as UV filter and carrier for cosmetic actives*

2007 NSTI Nanotechnology Conference and Trade Show - NSTI Nanotech 2007, Technical Proceedings.

Arya, N., Chakraborty, S., Dube, N., & Katti, D. S. (2009). Electrospraying: A facile technique for synthesis of chitosan-based micro/nanospheres for drug delivery applications. *Journal of Biomedical Materials Research Part B: Applied Biomaterials, 88B*(1), 17-31.

Badwan, A., Rashid, I., Omari, M., & Darras, F. (2015). Chitin and Chitosan as Direct Compression Excipients in Pharmaceutical Applications. *Marine drugs, 13*(3), 1519-1547.

Barras, A., Mezzetti, A., Richard, A., Lazzaroni, S., Roux, S., Melnyk, P., Betbeder, D., & Monfilliette-Dupont, N. (2009). Formulation and characterization of polyphenol-loaded lipid nanocapsules. *International Journal of Pharmaceutics, 379*(2), 270-277.

Bock, N., Dargaville, T. R., & Woodruff, M. A. (2012). Electrospraying of polymers with therapeutic molecules: State of the art. *Progress in Polymer Science, 37*(11), 1510-1551.

Cross, M. M. (1970). Viscosity, molecular weight and chain entanglement. *Polymer, 11*(5), 238-244.
Chakraborty, S., Liao, I. C., Adler, A., & Leong, K. W. (2009). Electrohydrodynamics: A facile technique to fabricate drug delivery systems. *Advanced Drug Delivery Reviews, 61*(12), 1043-1054.
Cheung, R. C. F., Ng, T., Wong, J., & Chan, W. (2015). Chitosan: An Update on Potential Biomedical and Pharmaceutical Applications. *Marine drugs, 13*(8), 5156-5186.
Dhiman, R. K. (2011). The Green Tea Polyphenol, Epigallocatechin-3-Gallate (EGCG)—One Step Forward in Antiviral Therapy Against Hepatitis C Virus. *Journal of Clinical and Experimental Hepatology, 1*(3), 159-160.
Elizaquível, P., Azizkhani, M., Aznar, R., & Sánchez, G. (2013). The effect of essential oils on norovirus surrogates. *Food Control, 32*(1), 275-278.
Estevinho, B., Rocha, F., Santos, L., & Alves, A. (2013). Microencapsulation with chitosan by spray drying for industry applications – A review. *Trends in Food Science & Technology, 31*(2), 138-155.
Fathi, M., Martin, A., & McClements, D. J. (2014). Nanoencapsulation of food ingredients using carbohydrate based delivery systems. *Trends in Food Science & Technology, 39*(1), 18-39.
Fu, N., Zhou, Z., Jones, T. B., Tan, T. T., Wu, W. D., Lin, S. X., Chen, X. D., & Chan, P. P. (2011). Production of monodisperse epigallocatechin gallate (EGCG) microparticles by spray drying for high antioxidant activity retention. *International Journal of Pharmaceutics, 413*(1-2), 155-166.
Geng, X., Kwon, O.-H., & Jang, J. (2005). Electrospinning of chitosan dissolved in concentrated acetic acid solution. *Biomaterials, 26*(27), 5427-5432.
Ghorani, B., & Tucker, N. (2015). Fundamentals of electrospinning as a novel delivery vehicle for bioactive compounds in food nanotechnology. *Food Hydrocolloids, 51*, 227-240.
Gómez-Mascaraque, L. G., Lagarón, J. M., & López-Rubio, A. (2015). Electrosprayed gelatin submicroparticles as edible carriers for the encapsulation of polyphenols of interest in functional foods. *Food Hydrocolloids, 49*(0), 42-52.
Gómez-Mascaraque, L. G., & López-Rubio, A. (2016). Protein-based emulsion electrosprayed micro- and submicroparticles for the encapsulation and stabilization of thermosensitive hydrophobic bioactives. *Journal of Colloid and Interface Science, 465*, 259-270.
Gómez-Mascaraque, L. G., Soler, C., & López-Rubio, A. (2016). Stability and bioaccessibility of flavonoids within edible micro-hydrogels. Chitosan vs. gelatin, a comparative study. *Food Hydrocolloids, In press*.
Homayoni, H., Ravandi, S. A. H., & Valizadeh, M. (2009). Electrospinning of chitosan nanofibers: Processing optimization. *Carbohydrate Polymers, 77*(3), 656-661.
Ishihara, M. (2015). A review on biomedical applications of chitosan-based biomaterials. *International Journal of Pharma and Bio Sciences, 6*(3), P162-P178.
Iversen, C., Kjøniksen, A.-L., Nyström, B., Nakken, T., Palmgren, O., & Tande, T. (1997). Linear and nonlinear rheological responses in aqueous systems of hydrophobically modified chitosan and its unmodified analogue. *Polymer Bulletin, 39*(6), 747-754.
Jaworek, A., & Sobczyk, A. T. (2008). Electrospraying route to nanotechnology: An overview. *Journal of Electrostatics, 66*(3–4), 197-219.
Jiménez-Martín, E., Gharsallaoui, A., Pérez-Palacios, T., Carrascal, J., & Rojas, T. (2014). Suitability of using monolayered and multilayered emulsions for microencapsulation of ω-3 fatty acids by spray drying: Effect of storage at different temperatures. *Food and Bioprocess Technology, 8*(1), 100-111.
Jimtaisong, A., & Saewan, N. (2014). Utilization of carboxymethyl chitosan in cosmetics. *International journal of cosmetic science, 36*(1), 12-21.
Kasaai, M. R. (2007). Calculation of Mark–Houwink–Sakurada (MHS) equation viscometric constants for chitosan in any solvent–temperature system using experimental reported viscometric constants data. *Carbohydrate Polymers, 68*(3), 477-488.

562 Khor, E., & Lim, L. Y. (2003). Implantable applications of chitin and chitosan. *Biomaterials,*
563 *24*(13), 2339-2349.
564 Larsen, C. A., & Dashwood, R. H. (2009). Suppression of Met activation in human colon cancer
565 cells treated with (−)-epigallocatechin-3-gallate: Minor role of hydrogen peroxide. *Biochemical*
566 *and Biophysical Research Communications, 389*(3), 527-530.
567 Larsen, C. A., & Dashwood, R. H. (2010). (−)-Epigallocatechin-3-gallate inhibits Met signaling,
568 proliferation, and invasiveness in human colon cancer cells. *Archives of Biochemistry and*
569 *Biophysics, 501*(1), 52-57.
570 López-Rubio, A., & Lagaron, J. M. (2012). Whey protein capsules obtained through
571 electrospraying for the encapsulation of bioactives. *Innovative Food Science & Emerging*
572 *Technologies, 13*(0), 200-206.
573 Luo, Y., & Wang, Q. Recent Advances of Chitosan and Its Derivatives for Novel Applications in
574 Food Science. *J Food Processing & Beverages, 1*(1), 13.
575 Maeng, Y.-J., Choi, S.-W., Kim, H. O., & Kim, J.-H. (2010). Culture of human mesenchymal stem
576 cells using electrosprayed porous chitosan microbeads. *Journal of Biomedical Materials*
577 *Research Part A, 92A*(3), 869-876.
578 Pancholi, K., Ahras, N., Stride, E., & Edirisinghe, M. (2009). Novel electrohydrodynamic
579 preparation of porous chitosan particles for drug delivery. *Journal of Materials Science:*
580 *Materials in Medicine, 20*(4), 917-923.
581 Park, J. H., Saravanakumar, G., Kim, K., & Kwon, I. C. (2010). Targeted delivery of low molecular
582 drugs using chitosan and its derivatives. *Advanced Drug Delivery Reviews, 62*(1), 28-41.
583 Pérez-Masiá, R., Lagaron, J., & Lopez-Rubio, A. (2015). Morphology and Stability of Edible
584 Lycopene-Containing Micro- and Nanocapsules Produced Through Electrospraying and Spray
585 Drying. *Food and Bioprocess Technology, 8*(2), 459-470.
586 Pérez-Masiá, R., Lagaron, J., & López-Rubio, A. (2014). Development and Optimization of Novel
587 Encapsulation Structures of Interest in Functional Foods Through Electrospraying. *Food and*
588 *Bioprocess Technology, 7*(11), 3236-3245.
589 Pérez-Masiá, R., López-Nicolás, R., Periago, M. J., Ros, G., Lagaron, J. M., & López-Rubio, A.
590 (2015). Encapsulation of folic acid in food hydrocolloids through nanospray drying and
591 electrospraying for nutraceutical applications. *Food Chemistry, 168*, 124-133.
592 Re, R., Pellegrini, N., Proteggente, A., Pannala, A., Yang, M., & Rice-Evans, C. (1999).
593 Antioxidant activity applying an improved ABTS radical cation decolorization assay. *Free*
594 *Radical Biology and Medicine, 26*(9–10), 1231-1237.
595 Rencher, A. C. (1992). Interpretation of Canonical Discriminant Functions, Canonical Variates,
596 and Principal Components. *The American Statistician, 46*(3), 217-225.
597 Ribeiro, M. P., Espiga, A., Silva, D., Baptista, P., Henriques, J., Ferreira, C., Silva, J. C., Borges, J.
598 P., Pires, E., Chaves, P., & Correia, I. J. (2009). Development of a new chitosan hydrogel for
599 wound dressing. *Wound Repair and Regeneration, 17*(6), 817-824.
600 Sang, S., Lee, M.-J., Hou, Z., Ho, C.-T., & Yang, C. S. (2005). Stability of Tea Polyphenol (−)-
601 Epigallocatechin-3-gallate and Formation of Dimers and Epimers under Common Experimental
602 Conditions. *Journal of Agricultural and Food Chemistry, 53*(24), 9478-9484.
603 Shenoy, S. L., Bates, W. D., Frisch, H. L., & Wnek, G. E. (2005). Role of chain entanglements on
604 fiber formation during electrospinning of polymer solutions: good solvent, non-specific
605 polymer–polymer interaction limit. *Polymer, 46*(10), 3372-3384.
606 Singh, B. N., Shankar, S., & Srivastava, R. K. (2011). Green tea catechin, epigallocatechin-3-
607 gallate (EGCG): Mechanisms, perspectives and clinical applications. *Biochemical Pharmacology,*
608 *82*(12), 1807-1821.
609 Singh, M. N. (2010). Microencapsulation: A promising technique for controlled drug delivery.
610 *Research in Pharmaceutical Sciences, 5*(2), 65-77.
611 Singh, R., Akhtar, N., & Haqqi, T. M. (2010). Green tea polyphenol epigallocatechi3-gallate:
612 Inflammation and arthritis. *Life Sciences, 86*(25-26), 907-918.

Sosnik, A. (2014). Production of drug-loaded polymeric nanoparticles by electrospraying technology. *Journal of biomedical nanotechnology, 10*(9), 2200-2217.
Steinmann, J., Buer, J., Pietschmann, T., & Steinmann, E. (2013). Anti-infective properties of epigallocatechin-3-gallate (EGCG), a component of green tea. *British journal of pharmacology, 168*(5), 1059-1073.
Su, Y. L., Leung, L. K., Huang, Y., & Chen, Z. Y. (2003). Stability of tea theaflavins and catechins. *Food Chemistry, 83*(2), 189-195.
Sun, K., & Li, Z. H. Preparations, properties and applications of chitosan based nanofibers fabricated by electrospinning. *Express Polymer Letters, 5*(4), 342-361.
Sun, N., Wang, J., Ji, L., Hong, S., Dong, J., Guo, Y., Zhang, K., & Pei, R. (2015). A Cellular Compatible Chitosan Nanoparticle Surface for Isolation and In Situ Culture of Rare Number CTCs. *Small, 11*(40), 5444-5451.
Tapia-Hernández, J. A., Torres-Chavez, P. I., Ramirez-Wong, B., Rascon-Chu, A., Plascencia-Jatomea, M., Barreras-Urbina, C. G., Rangel-Vázquez, N. A., & Rodríguez-Felix, F. (2015). Micro- and Nano-Particles by Electrospray: Advances and Applications in Foods. *Journal of Agricultural and Food Chemistry*.
Varshosaz, J. (2007). The promise of chitosan microspheres in drug delivery systems.
Wang, R., Zhou, W., & Wen, R.-a. H. (2006). Kinetic study of the thermal stability of tea catechins in aqueous systems using a microwave reactor. *Journal of Agricultural and Food Chemistry, 54*(16), 5924-5932.
Wang, W., Bo, S., Li, S., & Qin, W. (1991). Determination of the Mark-Houwink equation for chitosans with different degrees of deacetylation. *International Journal of Biological Macromolecules, 13*(5), 281-285.
Wang, X.-X., Ju, X.-J., Sun, S.-X., Xie, R., Wang, W., Liu, Z., & Chu, L.-Y. (2015). Monodisperse erythrocyte-sized and acid-soluble chitosan microspheres prepared via electrospraying. *RSC Advances, 5*(43), 34243-34250.
Xiao, X. (2008). Antiviral effect of epigallocatechin gallate (EGCG) on influenza A virus. *China journal of Chinese materia medica, 33*(22), 2678-2682.
Yunoki, A., Tsuchiya, E., Fukui, Y., Fujii, A., & Maruyama, T. (2014). Preparation of Inorganic/Organic Polymer Hybrid Microcapsules with High Encapsulation Efficiency by an Electrospray Technique. *ACS applied materials & interfaces, 6*(15), 11973-11979.
Zaki, N. (2014). Progress and Problems in Nutraceuticals Delivery. *J Bioequiv Availab, 6*, 075-077.
Zamani, M., Prabhakaran, M. P., & Ramakrishna, S. (2013). Advances in drug delivery via electrospun and electrosprayed nanomaterials. *International journal of nanomedicine, 8*, 2997.
Zhang, S., & Kawakami, K. (2010). One-step preparation of chitosan solid nanoparticles by electrospray deposition. *International Journal of Pharmaceutics, 397*(1–2), 211-217.
Zivanovic, S., Davis, R., & Golden, D. (2014). Chitosan as an antimicrobial in food products. *Handbook of Natural Antimicrobials for Food Safety and Quality*, 153.

Highlights

- Mw – concentration combinations for stable chitosan electrospraying are limited
- Viscosity, surface tension and conductivity help predicting morphology of materials
- EGCG microencapsulated in selected electrosprayed chitosan with 80% efficiency
- Encapsulation prolonged antiviral activity of EGCG against MNV

Supplementary Material

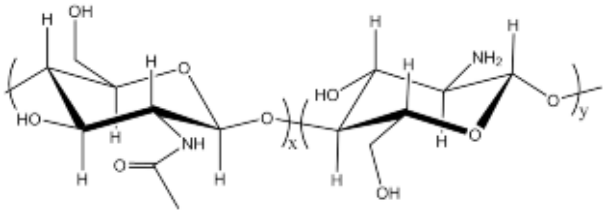

Figure S1. Schematic chemical structure of chitosan.

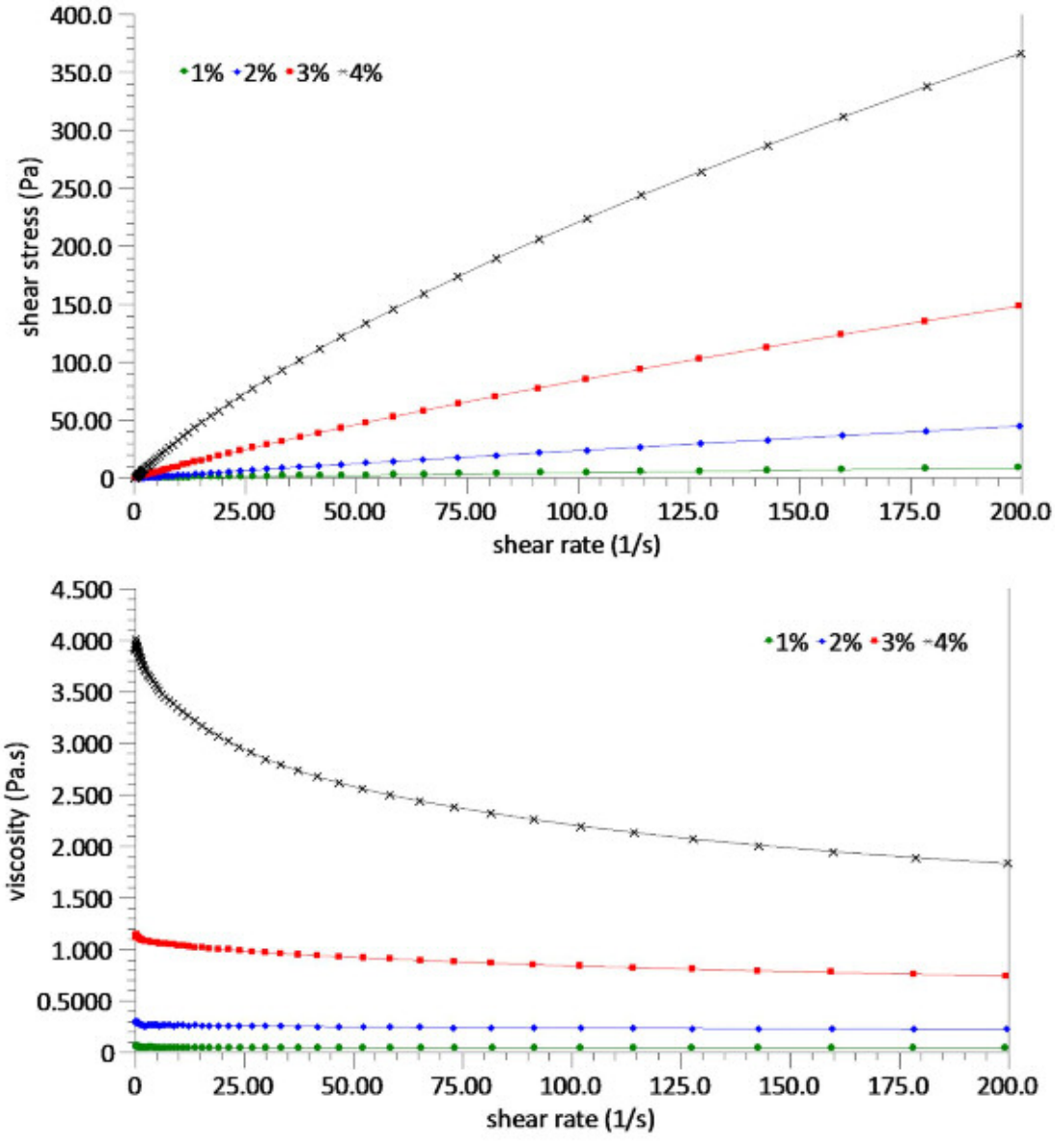

Figure S2. Rheological profiles (shear stress and viscosity *vs*. shear rate) for solutions of the chitosan with a Mw of 150 kDa in 90% acetic acid and different concentrations (1-4% w/v).

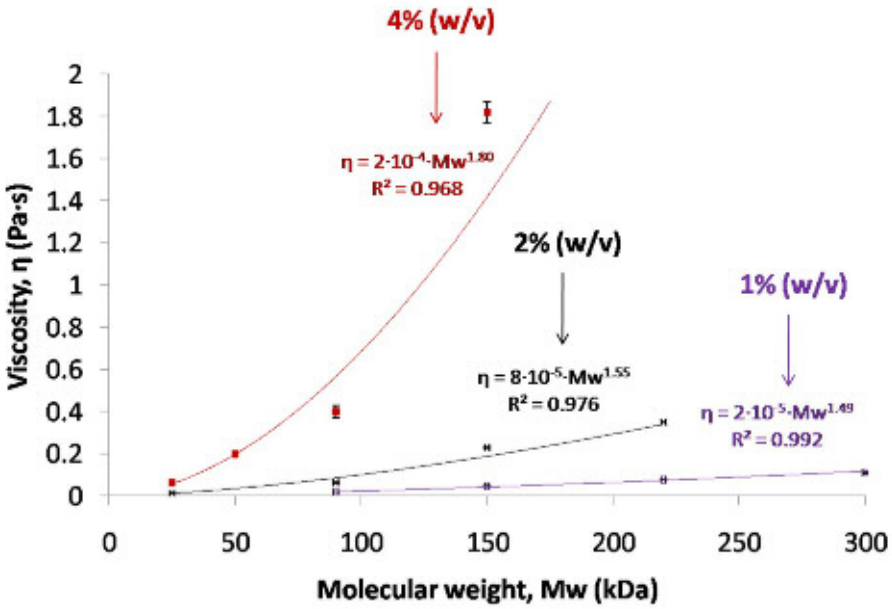

Figure S3. Viscosity of chitosan solutions as a function of the mean molecular weight for different concentrations.

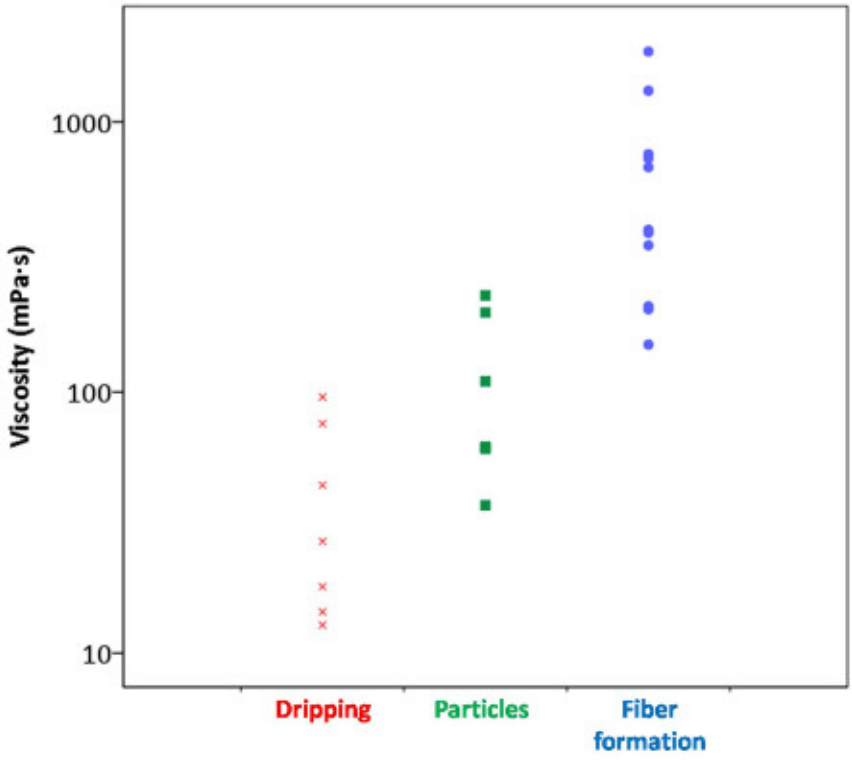

Figure S4. Experimental values of the viscosity (at 200 s^{-1}) of chitosan solutions giving rise to each of the obtained morphologies.

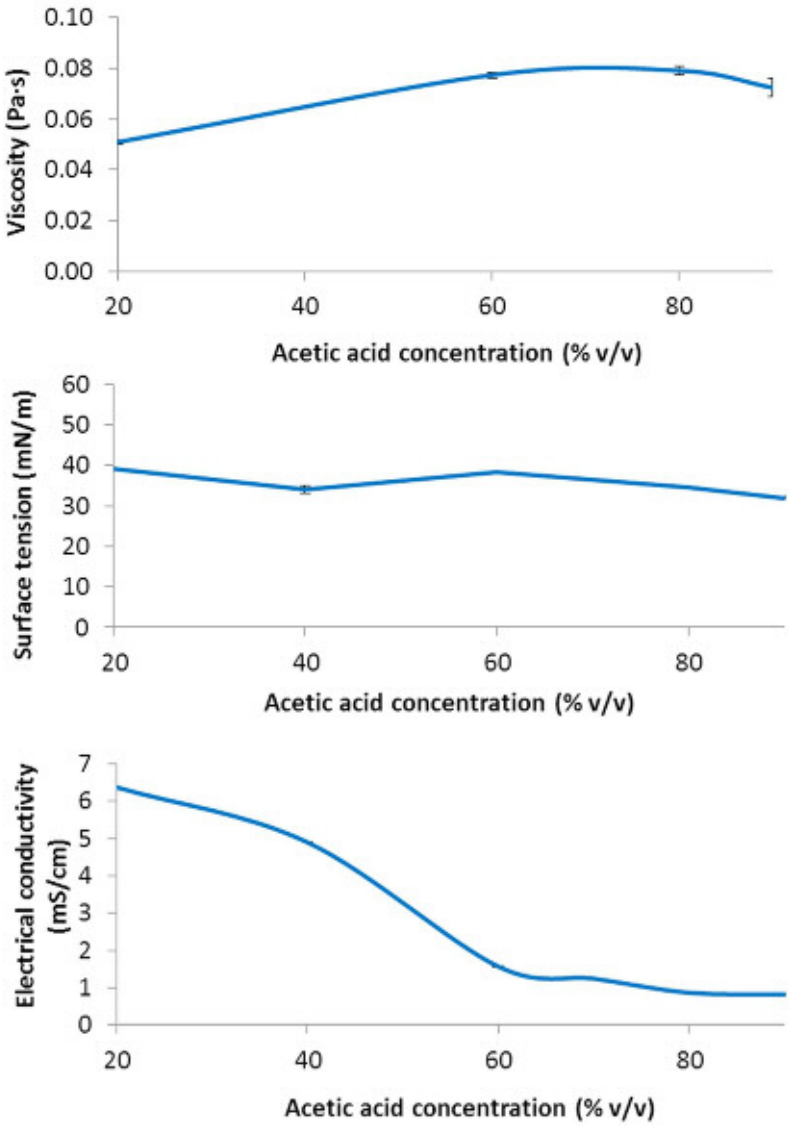

677

678 **Figure S5**. Viscosity, surface tension and electrical conductivity of chitosan solutions

679 (25 kDa, 5% w/v) as a function of the acetic acid concentration in the solvent.

680

681